CARS Measurements in the Near-Wake Region of an Axisymmetric Bluff-Body Combustor

G. L. Switzer,* L. P. Goss,† and D. D. Trump‡
Systems Research Laboratories, Inc., Dayton, Ohio
and
C. M. Reeves,§ J. S. Stutrud,§ R. P. Bradley,¶ and W. M. Roquemore**
U.S. Air Force Wright Aeronautical Laboratories, Wright-Patterson AFB, Ohio

The coherent anti-Stokes Raman spectroscopy (CARS) technique has been employed to measure temperatures in the near-wake recirculating flow region of a bluff-body-stabilized diffusion flame. Time-averaged temperature profiles and probability distribution functions are discussed in terms of the flowfield characteristics. Velocity information obtained by laser Doppler anemometry and the theoretical predictions of temperature and velocity are employed as aids in interpreting the time-averaged CARS data. Results of temperature measurements made with CARS and thermocouples of three different designs are compared. Several problems affecting CARS in the fuel-rich regions are identified and discussed. Among these are the effects of nonresonant background CARS generation, beam steering, and detector aging.

Introduction

RESULTS of coherent anti-Stokes Raman spectroscopy (CARS) diagnostic experiments being conducted in a simulated practical combustor environment at the Combustion Research Facility of the U.S. Air Force Wright Aeronautical Laboratories/Aero Propulsion Laboratory have been reported previously.[1,2] The research objectives and the facilities assembled to conduct this research have also been documented.[3,4] The published CARS results were obtained in a highly sooting bluff-body-stabilized diffusion flame at a position well downstream of the recirculation zone established by the bluff-body combustor. It was felt that both the CARS and thermocouple measurement techniques would be most applicable in this combustion zone; indeed, results of the averaged-temperature measurements are in good agreement for the two techniques.[2]

The CARS diagnostics efforts discussed here are a continuation of these experiments through examination of the near-wake region behind the bluff body where intense mixing occurs. During this study, two effects crucial to the CARS and probe diagnostic capability in this flame environment were identified. The first involved the effect upon the CARS temperature measurements of the contribution of the nonresonant background CARS signal generated from the unburned propane fuel; although several other problems were encountered that influenced the CARS results, this was the most severe. Even after nonresonant background effects and other CARS-related problems were minimized, a discrepancy between the CARS and thermocouple probe temperatures remained. The second effect upon the diagnostic capability was the intrusive nature of the thermocouple probe, which is believed to be responsible for the remaining tempeature discrepancy. The consequences of the physical body of a thermocouple probe disturbing or having secondary effects upon the temperature measurement process were examined by comparing results obtained with probes of several different geometries.

This paper identifies the problems influencing the CARS and thermocouple temperature diagnostic capabilities in the fuel-rich recirculation zone encountered during this measurement program and discusses the implemented solutions. CARS temperature profiles are presented and compared with those of thermocouples and model predictions. Flow velocities obtained from laser Doppler anemometry (LDA) data and model predictions are employed along with temperature probability distribution functions (pdf) as aids in interpreting the processes thought to be ocurring in the recirculation zone.

Combustion Tunnel Facility

The axisymmetric bluff-centerbody research combustor, as configured for these experiments, is diagrammed in Fig. 1. The centerbody is 79 cm long and has a diameter D of 14 cm. Gaseous propane fuel is injected from the center of the bluff-body face through a nozzle 4.8 mm in diameter. Annular airflow is conditioned using a honeycomb flow straightener and screens. The centerbody is mounted in a 25.4 cm diameter duct

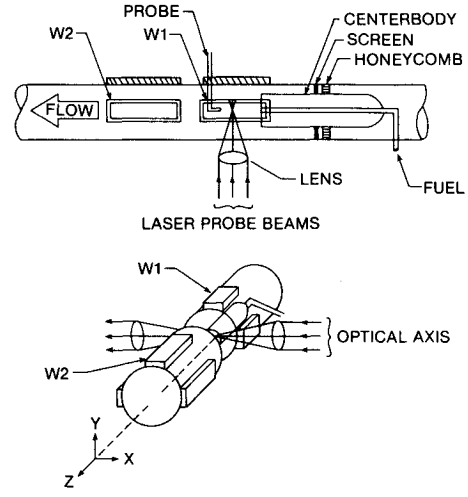

Fig. 1 Combustion tunnel, centerbody combustor, and probe arrangements.

Presented as Paper 85-1106 at the AIAA/SAE/ASME 21st Joint Propulsion Conference, Monterey, CA, July 8-10, 1985; received July 22, 1985; revision received Nov. 25, 1985.

*Senior Engineer. Member AIAA.
†Senior Chemist. Member AIAA.
‡Project Engineer.
§Project Engineer, Aero Propulsion Laboratory.
¶Senior Engineer, Aero Propulsion Laboratory.
**Senior Research Scientist, Aero Propulsion Laboratory.

equipped with 30.5 × 7.6 cm viewing ports that provide either probe or optical access to the combustion regions. To facilitate optical access, these ports are covered with 2.5 cm thick optical windows; metal ports are used for probe access. Additional details of the combustion tunnel facility can be found in Ref. 3.

All of the experiments were conducted under one set of test conditions. The annulus air velocity was 23.3 m/s, which corresponds to a Reynolds number of 1.5×10^6 based on the bluff-body diameter and inlet temperature of 294 K. The gaseous propane fuel-jet exit velocity was 69.6 m/s, with a Reynolds number of 4.2×10^4 based on the jet diameter and inlet temperature of 400 K. This condition was chosen because of the understanding gained in previous high-speed motion picture flame studies of the flowfield[4,16] and the computations of Sturgess and Syed,[5] which suggest that the measured vortex shedding frequency observed under this condition is far removed from the calculated acoustical resonances of the tunnel.

Theoretical Predictions

Theoretical predictions are presented to aid in the understanding of the complex flowfield in the near-wake region of the bluff body. The predictions were made using a computer code (TEACH) developed at Imperial College as a tecahing aid and described in Ref. 6. The code uses a hybrid upwind finite differencing scheme to solve the Reynolds-averaged equations. Closure is obtained by using the k-ϵ turbulence model with the standard constants. A simple one-step chemical reaction is assumed. Flat velocity and turbulence intensity inlet profiles were used for boundary conditions. The computational grid had 41 axial nodes and 39 radial nodes and extended 4D downstream. Grid independence of the solution was not determined and no attempts were made to improve on the calculations, since the predictions are used primarily to give qualitative insights into the flowfield.

Instrumentation

Thermocouples

It is well recognized that probes can interfere with their environment to such an extent that the temperature at the point of measurement in the presence and absence of the probe can be quite different. This is particularly true in the combusting recirculation zone behind a bluff body. Since the direction of the flowfield changes dramatically with time and location (as will be shown later in Fig. 7), probes must be sufficiently small to minimize blockage and sufficiently sturdy to survive the high-temperature environment. It is not always clear how to configure the probe to accomplish this. In this study, three thermocouple probe designs were evaluated in the near-wake region of the bluff body.

Envelopes of the three designs are shown in Fig. 2. All have a sheath diameter of 4.76 mm near the tip. The portion of the NAT probe that is perpendicular to the tunnel centerline is 6.35 mm in diameter. These dimensions are large with respect to the 4.78 mm diameter of the fuel jet, but small in comparison to the diameter of the bluff body. Hence, one might expect all of the probes to interfere significantly with the flow near the fuel jet, but to a lesser extent farther downstream or removed from the jet flow. All three thermocouples are made from platinum alloys. Probes NAT and R4 are type R (platinum-platinum/13% rhodium) thermocouples and POLST is a type S (platinum-platinum/10% rhodium). NAT, R4, and POLST are the identifiers used in the management of the acquired data.

The POLST probe in Fig. 2a was designed to minimize the effects of the stem. It is uncooled and has an exposed tip made from 22 gage wire with a 1.6 mm bead. The NAT probe in Fig. 2b is a shielded thermocouple with a platinum alloy sheath constructed in the shape of a rotated T. Hot gases pass over the 1.1 mm bead of the 24 gage thermocouple and exit through holes in the shield. The stem is water cooled to a distance of about 3 cm above the thermocouple where the platinum tip is located. The extension of the probe below the thermocouple has been shown to be beneficial in establishing symmetry in temperature measurements made in parabolic flows, while experience has shown that the end-on design of probe R4 (Fig. 2c) causes the peak temperature in a radial profile to shift away from the direction of the stem. R4 is an uncooled bare-wire thermocouple (20 gage) with a 1.4 mm bead.

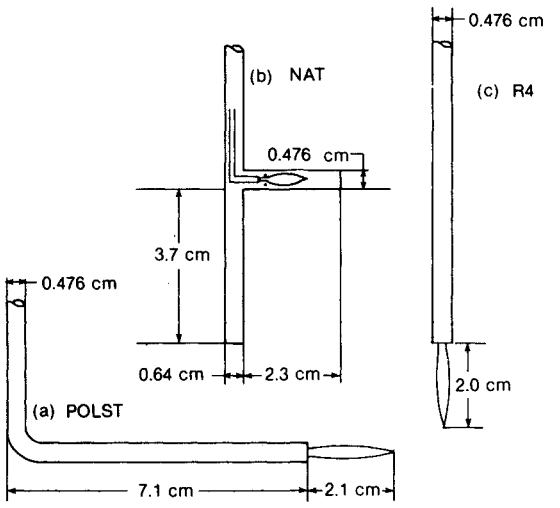

Fig. 2 Three thermocouple configurations used for temperature comparison: a) uncooled right-angle tip (POLST); b) water-cooled, T-shape tip (NAT); c) uncooled end-on tip (R4).

LDA System

The velocity data presented in this paper were obtained by Lightman et al.[7] using a two-component laser Doppler anemometer (LDA) especially designed for use in the combustion tunnel facility. It is a real-fringe system with a three-beam optical configuration and a fringe spacing of 10 μm. The scattered light is collected 10 deg from the forward direction by a parabolic mirror. The length of the measurement volume is 3 mm. Polarization is used to distinguish the two orthogonal velocity components. The optical beam, which is common to both LDA channels, is frequency shifted to permit measurement of both the positive and negative velocities. The scattered light is separated according to polarization and transmitted through optical fibers to two photomultipliers. The electrical signals are processed by two model 1990 TSI counter processors. Each velocity realization is stored in the facility computer for future processing.

Both the annulus air and the fuel were seeded with alumina particles using fluidized-bed seeders. For each point measurement, 5000 velocity realizations were obtained. In practice, it is very difficult to provide equal seed densities to the fuel and air streams and no attempt was made to do so for these measurements. Experiments in cold flows, where the extreme variations in the results were obtained by the use of one seeder and then the other, indicated that the precision of the velocity measurements was about 10%, except near the stagnation regions where much larger errors can occur. The precision was not determined for the combusting flow. A detailed description of the LDA system and the test procedures are given in Ref. 7.

Radial profiles of axial velocity are presented for axial locations at 4 and 8 cm. These data are not sufficiently detailed to describe the combustion flowfield in the near-wake region of the bluff body. However, they do provide insight that aids in interpreting the CARS temperature data and also lend credibility to the trends of the theoretical predictions.

CARS System

A detailed description of the optical and electronic configuration of the basic CARS system employed in these experiments can be found elsewhere.[1,8] Several modifications to the basic system were made for the present study. The CARS system employs a frequency-doubled neodymium-YAG laser that produces a 6 ns (FWHM) pulse at a 10 Hz repetition rate. A planar BOXCARS[9] optical configuration was employed in conjunction with a broadband N_2 Stokes dye laser to obtain single-shot N_2 temperature information along a 1.5 mm path in a spatial volume on the order of 1 mm^3. A beam expansion telescope was added to decrease the energy density of the ω_1 pump beams as they pass through the combustion tunnel access windows. This modification allowed a radial scan range sufficient to probe the total combusting flow plus the major portion of the annual airflow without causing damage to the window material.

The CARS signal generated in the sampled volume is collected in a 200 μm diameter fiber-optic transmission line and introduced into a 0.64 m spectrometer. Dispersion of the CARS information within the spectrometer is accomplished with a 2400 g/mm holographic grating and detection of the resultant spectral content is provided by a Tracor-Northern model TN 6132 diode array rapid scan spectrometer (DARSS) detector head. The detector is an intensified, gateable, 1024 element silicon photodiode array that exhibits sufficient linearity that only one optical split of the CARS signal is required to accommodate the dynamic range enhancement scheme[10] necessary to follow the factor of 500 variation in signal intensity occurring within the turbulent combusting medium. This grating and detector represent the remaining modifications to the basic CARS system with respect to the 1200 g/mm grating and the TN 1223IG detector described previously.[1] This combination exhibits a hybrid Gaussian/Lorentzian slit function and produces an overall system resolution of 4.1 cm^{-1} HWHM.

Results and Discussion

The initial attempts to measure the temperature with CARS within the highly recirculating flow in the near-wake region of the bluff-body combustor resulted in indications that in some areas of the flame the temperatures were as much as 500 or 600 K higher than those measured with thermocouples. Inspection of the single-shot CARS spectra in those areas revealed that a large nonresonant CARS background signal was being generated and was contributing to the N_2 spectral signature. This background signal is primarily due to the nonresonant susceptibility of the high concentration of unburned propane. Since the least squares temperature-fitting procedure being employed to fit the CARS spectra is sensitive to frequency and resonant CARS spectral shape only, it became evident that many temperatures in the predominantly fuel-rich combustion environment were being fit artificially high.

For a more accurate prediction of the composite N_2 spectra being generated experimentally, a technique similar to that described by Hall and Boedecker[11] was incorporated into the temperature-fitting procedure. This technique provides for the expression of CARS intensities as a function of two independent parameters, namely, temperature and a concentration factor consisting of the ratio of N_2 concentration to background nonresonant susceptibility. This modification allows one to consider the relative effects due to the concentration of probe-to-background species rather than to assume a predominant resonant N_2 contribution and a constant, relatively small background component. The magnitude of the effect of the background concentration factor upon temperature determination is illustrated in Fig. 3. Here, the theoretical spectra with and without background concentration are fit to an experimentally observed spectrum. The extreme shift in the lower-wavenumber tail of the 1080 K spectrum of Fig. 3 relative to the 1430 K spectrum is due primarily to a decrease of ~77% in the magnitude of the concentration factor expected in a stoichiometric environment. The addition of this parameter to the temperature-reduction procedure necessitated only a slight modification to the existing software, but increased the time required for fitting a temperature to a single spectrum from 1 to 3 s on the MODCOMP Classic computer system.

The decrease in CARS temperatures obtained by fitting to the background concentration can be interpreted in terms of the characteristic shape of the temperature pdf of Fig. 4. Here, the temperature pdf at a point 40 cm downstream of the combustor face is shown without (Fig. 4a) and with (Fig. 4b) consideration of background susceptibility modification. It is apparent that the average temperature decrease from 911 to 844

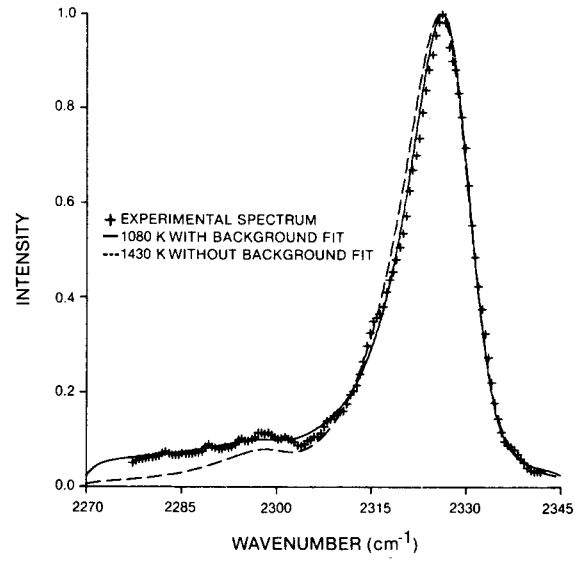

Fig. 3 Effect of background concentration on temperature fitting: + experimentally observed spectrum; — best fit at 1080 K, theoretical spectrum obtained with fitting to background concentration; —— best fit at 1430 K, theoretical spectrum without background variation.

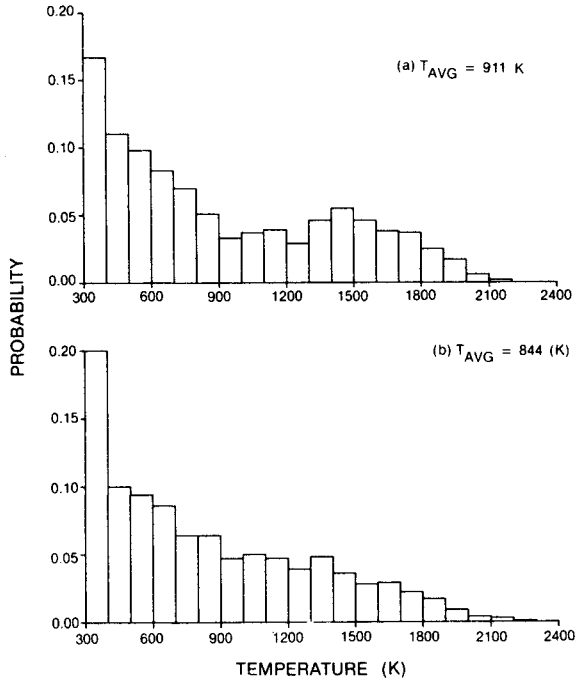

Fig. 4 Influence of background fitting procedure upon temperature pdf: a) distribution of temperatures without background fitting; b) temperature distribution when variable background is considered.

K results when the correction for background shifts the hotter temperatures in the 1500 K region to lower values. This shift in a relatively small number of temperature determinations has the effect of smoothing the pdf profile, thus making the aparent bimodal structure much less dominant. The magnitude of the shift in average temperature and the distortions in the pdf resulting from background considerations can be interpreted as a measure of the degree of penetration of combustion reactants within the combustion region.

Another phenomenon that affected the CARS temperature measurements was observed within the Tracor-Northern 6132 detector. It was observed that a relatively short-duration overexposure of the diode array resulted in a permanent nonuniform decrease in the sensitivity of the affected diodes. One of the consequences of this desensitization was that the spectral profiles were artificially broadened, thus producing an apparent increase in temperature. This effect was especially noticeable at lower temperatures where the spectral width is most critical in temperature fitting. For instance, what normally would have been a 400 K spectrum could be distorted to indicate a temperature 150-200 K higher.

Since overexposure of the detector diodes is unavoidable at present, particularly near the edge of the flame in a turbulent combustion environment, several steps were taken to minimize its potential effect. The sampled spectra were moved to new areas of the 1024 element array having uniform response and sensitivity. Subsequent overexposure time of the detector was kept to a minimum by input filtering. Daily calibration to room temperature and to a standard flame provided a check for variation in detector sensitivity. These steps effectively eliminated the influence of detector "aging" upon the measurement process and helped to ensure the reliability of the CARS data.

In addition to its nonresonant contribution to the CARS spectral information, the fuel-rich combustion environment in the near-wake region of the flame presents another problem in CARS diagnostics. Large thermally induced gradients in the index of refraction are present between the mixing cold fuel and the hot combustion products. These gradients cause considerable bending of the optical beams in transit through the flame. Since each of the three laser beams (two of frequency ω_1 and one at frequency ω_2) entering the sample focal volume experiences a different optical path, each is steered independently and there is relative movement at the beam cofocus. This defocusing causes a decrease in CARS intensity. While this intensity does not detract from the spectral content (i.e., temperature-dependent information), it does prohibit determination of N_2 concentration by relative intensities.[8] Thus, until a scheme for compensation of turbulent beam steering can be implemented, the CARS concentration measurement capability will not be reliable for the near-wake recirculating combusting flow.

As stated earlier, a large discrepancy between temperatures determined by CARS and thermocouple probes remained after the CARS temperature-reducing procedure was modified to fit nonresonant background contributions. To help identify the source of this discrepancy, the type, geometry, and orientation of the thermocouple were varied. Some of the results of these experiments are shown in Fig. 5. The radial profiles enable a comparison of the CARS temperatures to those obtained from the three thermocouple probes identified in Fig. 2. The NAT and POLST probes were oriented parallel to the flow, facing upstream. The R4 probe was inserted from the top and normal to the flow axis. The data of Fig. 5a reveal that the error between the CARS and NAT temperatures is due to the probe characteristics. The distinct departure of the NAT profile from the other thermocouple data suggests that this probe exhibits a large perturbing presence in the combusting media. The cause of this perturbation becomes apparent if one considers that, at an axial location of 4 cm, the combusting flow is highly recirculating, as will be discussed presently. Thus, the body of the NAT probe located downstream of the thermocouple tip plays a definite role in blocking the transport of the reverse-flowing combusting gases that would otherwise be present at the measurement location. Although the POLST and R4 probe temperature profiles of Fig. 5a are similar in shape, there is sufficient spread in the data to cause concern that perhaps one or both of these probes also perturb the characteristics of the measurement volume by their presence in a recirculating flowfield.

The four temperature profiles of Fig. 5b, obtained at an axial location of 24 cm, show a marked convergence. This convergence is thought to occur because this measurement location is downstream of the recirculation zone and, thus, the thermocouple is influenced to a lesser degree by the presence of the physical body of the probe. Secondary effects such as heat conduction away from the thermocouple through its leads or probe body and radiation from the heated probe body may contribute to the probe inaccuracies, but their effect is thought to be much less severe. The convergence of these profiles continues as the measurement location moves further downstream. At $z = 40$ cm, where the flow is parabolic, point-to-point temperature differences of less than 50 K between CARS and the NAT probe have been measured.[2]

Figure 6 shows measured and predicted radial profiles of average temperature, axial velocity, and rms velocity at axial locations of 4 and 8 cm. This figure is presented to illustrate the qualitative agreement between the TEACH code predic-

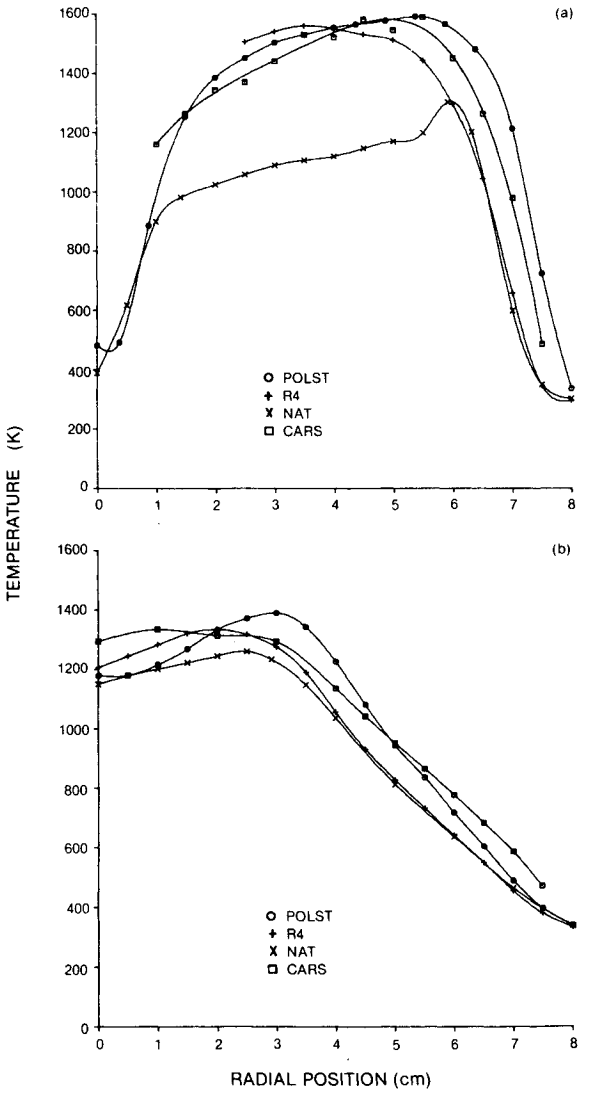

Fig. 5 Radial profile of temperature for CARS and thermocouples at axial locations of a) 4 cm (0.29 z/D) and b) 24 cm (1.71 z/D).

tions and experiment. It also offers insight into the processes that are occurring. It is our intent to give only a qualitative assessment of the TEACH code predictions since measured inlet conditions have not been used and the necessary checks on the numerical accuracy of the computations have not been made. It should be noted that if precise inlet conditions are desired, inlet velocity and turbulence intensity data for this combustor can be found in Ref. 4. Also, recent studies have shown that LDA velocity data, when not collected at a constant time interval, are Favre averaged (density weighted), whereas the TEACH predictions are time averaged.[13-15] This difference must be taken into account if quantitative assessments of the model are to be made.

Qualitative agreement between theory and experiment is most evident when comparing the temperature plots in Fig. 6. At $z=4$ cm, the temperature profile in Fig. 6a has a broad peak that is skewed away from the centeline for both prediction and measurement. At $z=8$ cm, the theoretical and measured temperature peaks in Fig. 6b are more rounded. The maximum temperature occurs at a radial location very near that of the zero-velocity point in both Figs. 6a and 6b. The breadth in the temperature profile and the radial location of the peak appear to be related to the width of the reverse-flow (negative-velocity) region. The TEACH code predicts and LDA measurements confirm that the reverse-flow region is considerably larger at $z=4$ cm than at $z=8$ cm. The radial locations of the peak temperature and the zero velocity are also farther from the centerline at the 4 cm location than at the 8 cm location. The change in width of the reverse-flow region with axial location is clearly evident from the velocity vector overlay in Fig. 7.

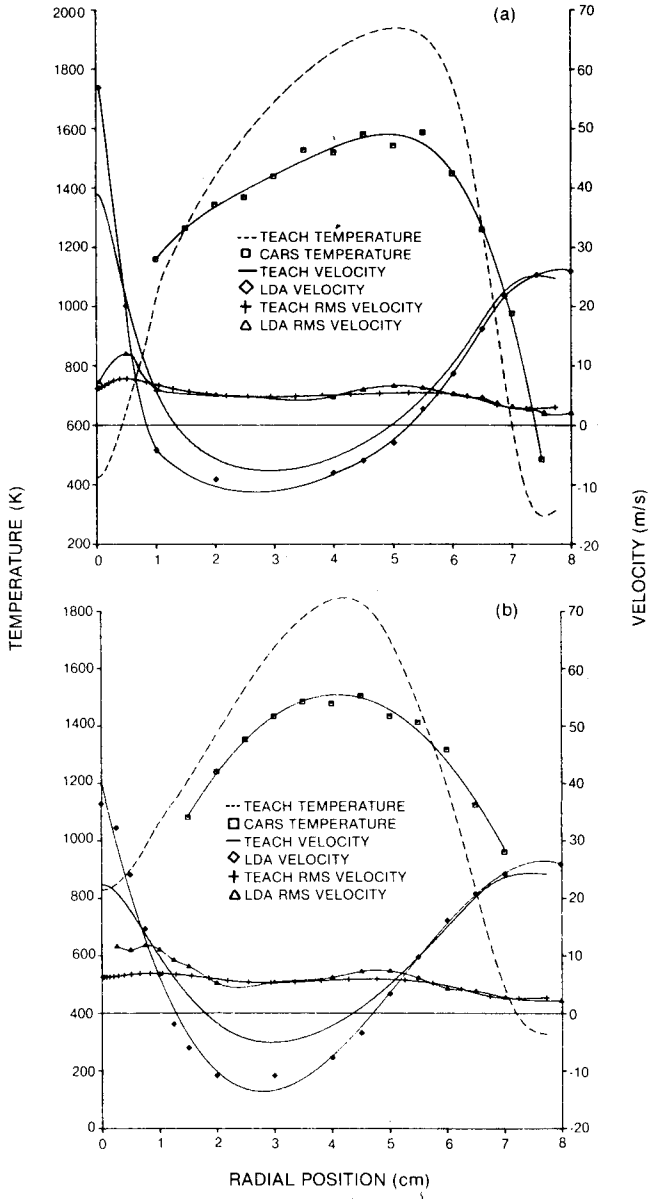

Fig. 6 Comparison of time-averaged CARS temperatures and averaged and rms LDA axial velocities with TEACH code predictions at axial locations of: a) $z=4$ cm (0.29 z/D) and b) $z=8$ cm (0.57 z/D).

The temperature decreases very rapidly at radial locations greater than the peak temperature location in both Figs. 6a and 6b. Since this occurs just as the flow changes direction, the rapid decay is most likely due to mixing of the cold downstream flowing annular air with hot products and burning fuel. This view is supported by the small peak in the measured rms velocity fluctuations, which indicates enhanced mixing near the outer velocity stagnation point. The TEACH code predictions also show a small peak in the rms velocity near the stagnation point. However, it is not very noticeable in Fig. 6 because of the chosen velocity scale. The TEACH code predictions of average and rms velocities and temperature appear to exhibit very good qualitative agreement with the measured data.

Measured and predicted temperature isotherms along with the predicted velocity field are shown in Fig. 7. The average CARS temperatures on a 0.5 cm radial by 2 cm axial grid (for $r=0$-7 cm and $z=2$-26 cm) were used to produce the upper half of the temperature contour plot. For purposes of comparison and to assist in interpretation, the TEACH code predictions of temperature and velocity are presented in the lower half of the figure. For the sake of clarity, some of the velocity vectors have been omitted from the fuel jet; otherwise, they would obscure the temperature isotherms in this region. Since the absolute temperatures measured using CARS and predicted by TEACH are different, the scale shown in Fig. 7 is normalized to the maximum temperature in each half (1587 K for CARS and 1994 K for predictions). This approach allows more convenient comparison of the qualitative features. Large toroidal vortex structures are known to be shed from the bluff body.[4] An illustration of the shed vortices is superimposed on the time-averaged flowfield calculation in Fig. 7 as a reminder that the dynamic events are important in discussing the processes occurring in the near-wake region of the bluff body.

The strong similarity between the CARS-measured and TEACH-predicted temperatures in Fig. 7 suggests that the predictions contain the important qualitative features of the entire temperature field. For example, each isotherm shows that the cool fuel is heated as it moves downstream and radially outward. Also, each map shows that there are two hot spots (labeled by their normalized temperature). The one located downstream and near the centerline will be referred to as the fuel-jet hot spot, and the other near the face of the bluff body will be called the annular-jet hot spot. The fuel jet hot spot identified in the CARS data is considerably cooler than that predicted by TEACH and is displaced farther downstream. This displacement differential might be expected because this hot spot is associated with the central jet and the TEACH code with the standard constants normally underpredicts the velocity field and overpredicts the development of a round jet flow.

Figure 7 shows that the TEACH code predicts the annular jet hot spot to be near the vortex center established by the annular jet. This is supported by the measured data in Fig. 6. The maximum temperature in the flowfield was measured at an axial location of 4 cm and is shown in Fig. 6a. As noted earlier, the measured peak temperature is very near the radial location where the measured axial velocity is zero. From observations of high-speed movies of the flame, it was determined that this position is very near the vortex center.[4]

The apparent connection between the velocity and temperature fields suggests that the dominant mechanism of

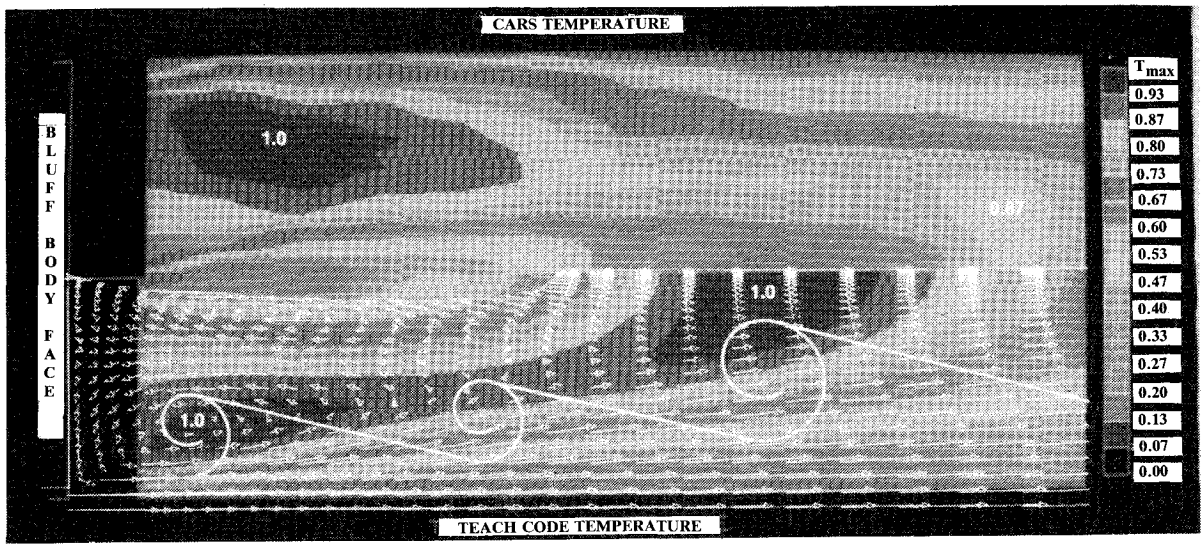

Fig. 7 Comparison of the time averaged CARS temperature measurements and TEACH predictions of temperature and velocity with an illustration of shed vortices.

heat transport is convection. An examination of the TEACH predictions showed that the magnitude of convective heat transport in the shear layer of the bluff body is at least an order of magnitude larger than that due to the turbulent diffusion transport at all but a few locations in the flowfield. The qualitative agreement between the predictions and experimental data suggests that the measured temperature field might also be interpreted in terms of the convective heat transfer. To this end, a qualitative explanation of the TEACH code predictions of the temperature field, based on the mean velocity field, will be presented as a reasonable interpretation of the time-averaged CARS data.

The zero axial velocity surface of the annular jet vortex, which is observed in the lower half of Fig. 7, is thought to be important for understanding the cause of the associated hot spot. Judging from the velocity plot, the zero axial velocity surface extends about one bluff-body diameter downstream. This surface, which is near the outer edge of the 0.80-0.87 isotherm, is considered to be very important because it separates the gases flowing upsteam from those flowing downstream. The fluid elements on either side of the surface haver very different time histories. The downstream flow, which is outside the surface, contains mostly cold annulus air and some hot products very near the surface. Inside the surface, the ignited fuel and hot products are convected upstream by the mean flow. Tracking the velocity vectors and isotherms near the fuel jet reveals that combustion is sustained in the upstream flow region by the continuous supply of hot fuel from the outer shear layer of the fuel jet. Also, the fuel transported near the zero velocity surface of the annular jet vortex must linger for a relatively long time because of the very low velocities. In effect, the long residence time ensures sustained high temperatures in this region.

The fuel jet hot spot, as noted in Fig. 7, is also located in a region where velocities are very low. The velocity vector plot in Fig. 7 shows that the fuel jet penetrates the recirculation zone established by the annular jet. Tracking the magnitude of the velocity vectors near the centerline reveals that as the fuel travels downstream, the velocity decays to a minimum value and then begins to increase. The fuel jet hot spot is located in this region of low velocity. Studies of high-speed movies of the flame also show that the fuel jet penetrates the recirculation zone and that the fuel jet hot spot is located in a region where the axial velocities are very low.[4]

The fuel jet is heated by the entrainment of hot products. The vortex associated with the central jet (see Fig. 7) also has a zero axial velocity surface that separates the fuel and hot products moving downstream from the products and reactants moving upstream. Some of the hot products moving upstream are entrained into the fuel jet near the bluff-body face, thus heating the fuel as it moves downstream. By the time the fuel near the centerline reaches minimum velocity, reaction has begun as a result of the entrained hot products. Since this burning fuel remains for a considerable time in this region where the velocity is low, the temperatures will be high. The TEACH predictions indicate that the radial extent of the downstream hot spot is determined by the cooling effects of the radial penetration of the annular jet shear layer. This can be confirmed by tracking the velocity vectors in the shear layer of the bluff body as they move downstream.

The discussions have considered a time-averaged view of the near-wake region. However, it must be remembered that the flow is very dynamic, with large toroidal vortices (illustrated in Fig. 7) being shed from the bluff body.[16] The impact of the dynamic motions on the temperature field is shown in Fig. 8. In this figure, each pdf is the result of averaging 6-8 sets of at least 1500 individual CARS temperature samples. The probability axis height is 0.2 and the temperature axis is 300-2400 K with 100 K temperature bin widths (same as Fig. 4). Temperature probabilities of 0.2-0.27 are represented by darkened bin segments and temperature bins exceeding a probability of 0.27 are clipped at 0.2 on the plot and labeled with their actual value. The worst-case precision of the experiment, as indicated by averaging six CARS data sets taken on different days in the shear layer of the annular jet, was 80 K. For most locations, the experiment was repeatable to 40 K. Those plots, consisting of a single line, indicate only "best-estimate" values of the thermocouple temperatures. CARS measurements were not made in these locations due to large nonresonant signal generation from the unburned propane in the fuel jet. The time-averaged and rms temperatures for the particular pdf are given in the upper right-hand corner of each plot.

The pdf's in Fig. 8 provide a map of the annular air transported into the near-wake region. The 300 K temperatures can serve as a marker for the annulus air that is unmixed and, thus, unheated by the combustion process. By tracking the radial locations where the probability of measuring 300 K temperatures approaches zero (from the high side), one can determine how far the annulus air extends into the near-wake region without being mixed. The probability of the 300 K bin yields the fraction of time during which this occurs. An examination of the pdf's for an axial location of 4 cm shows that, at a radial location of 5 cm or less, there is zero

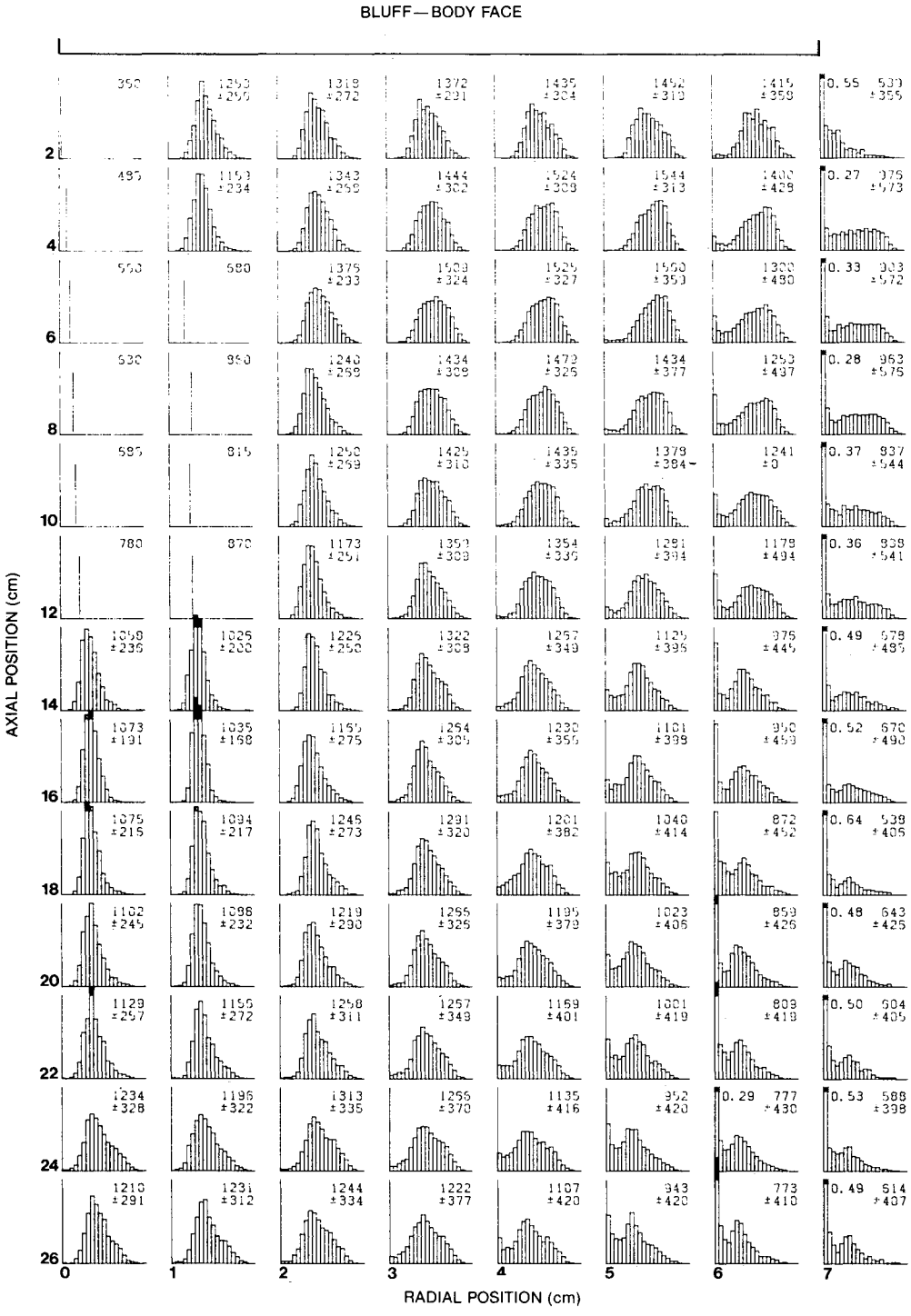

Fig. 8 CARS temperature pdf's in the near-wake region of the bluff body.

probability of measuring a temperature of 300 K whereas, at 6 and 7 cm, 300 K temperatures will be measured at certain times. This implies that the annular flow penetration into the near-wake region at $z=4$ cm is between 5 and 6 cm. Figure 6a confirms this, since the measured zero axial velocity location separating the downstream and upstream moving gases is at 5.3 cm. At the 8 cm axial location, the annular air does extend to the 5 cm radial location, as interpreted by the nonzero probability of measuring 300 K. The location of the zero axial velocity point is 4.7 cm, according to the LDA data in Fig. 6b. Thus, by tracking the probability of measuring a temperature of 300 K, one can determine to what extent unmixed annular air penetrates the near-wake region and the fraction of time during which it happens.

The temperature pdf's in Fig. 8 support the view, established by the study of high-speed movies in Ref. 16, that shed vortices are actually responsible for the transport of annular air and heat (mixed air and hot products) into the wake of the bluff body. The presence of the 300 K inlet temperatures at certain times and very high temperatures at other times indicates that the flow is intermittent. Indeed, the probability of observing the presence of annular air is a measure of the intermittence. The study of high-speed movies suggests that the cause of the intermittence is the occurrence of large-scale shed vortices. By imagining the observed large-scale vortices being convected downstream, as depicted in Fig. 7, one can more easily visualize the events leading to the transport of unmixed annular air into the near-wake region. As the vortex rolls up,

an interface separating annular air and products is formed. As the vortex is convected downstream, the rotational motion toward the centerline transports unmixed annular air at the interface deep into the shear layer of the bluff body. As the vortex continues to rotate, it transports reactants, hot products, and air radially outward. The biomodal shapes of the pdf's indicate the presence of these large toroidal vortices and their influence upon the temperature field.

High-speed movies of the flame indicate that the fuel is burned in discrete packets, surrounded by hot products and air.[16] Studies of high-speed movies of a laser sheet-lit view of a cold reacting flow in a vertically mounted centerbody suggest that the discrete packets of reacting fuel are vortices shed from the fuel jet.[17] The convection of these packets of burning fuel past the measurement point is also believed to be responsible in part for the shape of the temperature pdf's in Fig. 8.

Summary and Conclusions

CARS temperature measurements have been extended into the recirculating near-wake region of a bluff-body-stabilized diffusion flame. Corrections for nonresonant background due primarily to the presence of unburned fuel were required to obtain what is considered to be valid CARS data. Attempts to establish the accuracy of the measurements in this environment failed due to lack of a suitable standard technique for comparing time-averaged temperatures. Thermocouples, which have been used in the past to check the performance of averaged CARS temperature measurements in parabolic flows, perturbed the near-wake flowfield to such an extent that the data were unreliable. This was determined by making measurements with thermocouples of three different shapes.

CARS temperature pdf's were most useful in providing insight into the dynamic nature of the turbulent combustion processes occurring in the near-wake region of the bluff body. By tracking the probability of measuring the inlet air temperature, it was determined that unheated and unmixed annular air is transported into the near-wake region toward the peak time-averaged temperature and that the transport is intermittent. The bimodal shape of the temperature pdf's and previous studies of high-speed movies of the flame suggest that the transport mechanism of heat, air, and products in the shear layer of the bluff body is due to the convective nature of large-scale vortices shed from the bluff body.

A quantitative comparison of experimental results and TEACH code predictions was not attempted in this study because sufficient checks have not been made on the numerical accuracy of the calculations. However, the TEACH code did successfully predict many of the qualitative features of the mean temperature and axial velocity data. The success of the predictions is thought to be due to the fact that the TEACH-calculated radial convective transport is considerably larger at most locations in the shear layer of the bluff body than the calculated transport by turbulent diffusion via the eddy viscosity model. Also, it is very doubtful that the TEACH code will provide accurate quantitative predictions of the temperature field unless intermittency and mixing due to the large-scale shed vortices are taken into account.

Acknowledgments

The authors would like to thank Mr. M. Russell for assisting in the operation of the combustion tunnel and Lt. J. Doty and Ms. C. Obringer for their help in data reduction and analysis. We also express appreciation to Drs. R. Piccirelli, L. D. Chen, and D. R. Ballal for their useful discussions. Appreciation is extended to Ms. M. Whitaker for assisting with the figures and Ms. R. Bush for preparing the manuscript. This research was sponsored by the U.S. Air Force Wright Aeronautical Laboratories, Aero Propulsion Laboratory, under Contract F33615-80-C-2054, W.U. 30480502, with Systems Research Laboratories, Inc., and by the U.S. Air Force Office of Scientific Research, W.U. 2308S705.

References

[1]Switzer, G. L., Goss, L. P., Roquemore, W. M., Bradley, R. P., Schreiber, P. W., and Roh, W. B., "Application of CARS to Simulated Practical Combustion Systems," *Journal of Energy*, Vol. 4, 1980, pp. 209-215.

[2]Switzer, G. L., Trump, D. D., Goss, L. P., Roquemore, W. M., Bradley, R. P., Stutrud, J. S., and Reeves, C. M., "Simultaneous CARS and Luminoisty Measurements in a Bluff-Body Combustor," AIAA Paper 83-1481, June 1983.

[3]Roquemore, W. M., Bradley, R. P., Stutrud, J. S., Reeves, C. M., and Krishnamurthy, L., "Preliminary Evaluation of a Combustor for Use in Modeling and Diagnostic Development," ASME Paper 80-GT-93, March 1980.

[4]Roquemore, W. M., Bradley, R. P., Stutrud, J. S., Reeves, C. M., Obringer, C. A., and Britton, R. L., "Utilization of Laser Diagnostics to Evaluate Combustor Models," *Combustion Problems in Turbine Engines*, AGARD CP-333, Vol. 19, 1983, pp. 1151-1157.

[5]Sturgess, G. J. and Syed, S. A., "Dynamic Behavior of Turbulent Flow in a Widely-Spaced Co-Axial Jet Diffusion Flame Combustor" AIAA Paper 83-0575, Jan. 1983.

[6]Gosman, A. D. and Ideriah, F. J. K., "TEACH-T: A General Computer Program for Two-Dimensional Turbulent Recirculating Flows," Dept. of Mechanical Engineering, Imperial College, London, June 1976.

[7]Lightman, A., Magill, P. D., and Andrews, R. J., "Laser Diagnostics Development and Measurements and Modeling of Turbulent Flowfields of Jets and Wakes," AFWAL-TR-832044, Pt. 1, June 1983.

[8]Switzer, G. L. and Goss, L. P., "A Hardened CARS System for Temperature and Species-Concentration Measurements in Practical Combustion Environments," *Temperature: Its Measurement and Control in Science and Industry*, Vol. 5, edited by J. F. Schooley, American Institute of Physics, New York, 1982, pp. 583-587.

[9]Eckbreth, A. C., "BOXCARS Crossed-Beam-Phase-Matched CARS Generation in Gases," *Applied Physics Letters*, Vol. 32, 1978, pp. 421-423.

[10]Goss, L. P., Switzer, G. L., and Trump, D. D., "Temperature and Species Concentration Measurements in Turbulent Diffusion Flames by the CARS Technqiue," AIAA Paper 82-0240, Jan. 1982.

[11]Hall, R. J. and Boedicker, L. R., "CARS Thermometry in Fuel-Rich Combustion Zones," *Applied Optics*, Vol. 23, 1984, pp. 1340-1346.

[12]Sturgess, G. J., "Aerothermal Modeling Program—Phase I Final Report," NACA CR 168202, May 1983.

[13]Magill, P. D., Lightman, A. J., Orr, E. E., Bradley, R. P., and Roquemore, W. M., "Simultaneous Velocity and Emission Measurements in a Bluff-Body Combustor," AIAA Paper 82-0883, June 1982.

[14]Heitor, M. V., Taylor, A. M. K. P., and Whitelaw, J. H., "Simultaneous Velocity and Temperature Measurements in a Premixed Flame," *Experimental Measurements and Techniques in Turbulent Reactive and Non-Reactive Flows*, edited by R. M. C. So, J. H. Whitelaw, and M. Lapp, ASME AMD, Vol. 66, Dec. 1984, pp. 243-274.

[15]Goss, L. P., Trump, D. D., and Roquemore, W. M., "A Combined CARS/LDA Instrument for Simultaneous Temperature and Velocity Measurements," to be published.

[16]Roquemore, W. M., Bradley, R. P., Stutrud, J. S., Reeves, C. M., and Britton, R. L., "Influence of Vortex Shedding Process on a Bluff-Body Diffusion Flame," AIAA Paper 83-0335, Jan. 1983.

[17]Roquemore, W. M., Tankin, R. S., Chiu, H. H., and Lottes, S. A., "The Role of Vortex Shedding in a Bluff-Body Combustor," *Experimental Measurements and Techniques in Turbulent Reactive and Non-Reactive Flows*, edited by R. M. C. So, J. H. Whitelaw, and M. Lapp, ASME AMD, Vol. 66, Dec. 1984, pp. 159-174.